Probing Intermolecular Communication with Surface-Attached Pyrene

Maciej Mazur[†] and G. J. Blanchard*[,‡]

Department of Chemistry, Laboratory of Electrochemistry, University of Warsaw, 02-093 Warsaw, Pasteura 1, Poland, and Department of Chemistry, Michigan State University, East Lansing, Michigan 48824-1322

Received: October 13, 2004; In Final Form: December 20, 2004

We report on the covalent attachment of pyrene derivatives to solid substrates and their spectroscopic and electrochemical characterization. We have constructed several molecular assemblies attached to silica and indium-doped tin oxide surfaces where pyrene molecules are co-immobilized with other functionalities. It was shown that the addition of hydrophobic molecules to the pyrene-containing interface results in a significant decrease in the pyrene I_1/I_3 vibronic emission band ratio and an increase in the water drop contact angle due to increased hydrophobicity of the interface. The co-attachment of perylenedodecanoic acid, for which the absorption band overlaps with the emission spectrum of pyrene, shows significant intermolecular communication between these species. The co-immobilization of ferrocene serves as an effective fluorescence quencher for tethered pyrene. In all cases, our data point to significant intermolecular communication between adsorbate species, and the combination of spectroscopic and electrochemical interrogation provides insight into the loading density and local environment(s) characteristic of these interfaces.

Introduction

A wide range of present-day technologies, such as catalysis, chemical sensing, and nanoelectronics, rely on chemical and physical phenomena that proceed at interfaces. Because of the limited structural control we can exert over solid surfaces, one attractive strategy for the tailoring of interfaces for specific purposes is to deposit monolayer or multilayer structures onto these interfaces. Such adlayers can be prepared by any of several methods, with Langmuir−Blodgett and self-assembly techniques being the most useful and widely used approaches of effecting interface structural control.[1−5]

The chemical modification of interfaces requires the development and use of measurement techniques that are capable of probing the interfaces once formed. Both electrochemistry and spectroscopy have proven to be useful for this task, depending on the interface used. For both electrochemical and spectroscopic measurements, the incorporation of probe molecules into the modified interface serves to enhance sensitivity and specificity of the information gained from such measurements. Fluorescent spectroscopic probes have proven especially useful because they can be detected with high sensitivity and in selected cases the details of their emission profile are reflective of their immediate environment.[6−11]

We have chosen to use the well-characterized chromophore pyrene[12−17] as an optical probe for this work because of its ability to sense the "polarity" of its microenvironment through the intensity ratio of two emission bands. These two bands, the 0−0, I_1, and a vibronic transition between the vibrationless S_1 state and the ground state 1100 cm^{-1} b_{3g} vibrational mode, I_3, respond differently to the dielectric properties of the chromophore immediate environment. The resulting band ratio I_1/I_3 is used widely for the characterization of environmental "polarity".[7,18,19] For pyrene, the I_1/I_3 ratio varies from 0.6 for the most nonpolar solvents such as hexane to nearly 2 in polar solvents such as DMSO.[20] For substituted pyrenes, the emission band ratio environmental dependence is somewhat less sensitive owing to the reduction in symmetry of the substituted pyrene, but if chosen properly, substituted pyrenes can be used quite effectively as a probe of interface local environment.

We report here on intermolecular communication within several interfacial systems, both under conditions of surface structural heterogeneity and for immersion of the substrate in solvents of varying polarity. It was found that the co-immobilization of selected molecules with pyrene derivatives has a measurable effect on the spectral response of the pyrene chromophore, and the details of this effect depend on the identity of the surface modifier. We gauge the sensitivity of vibronic band intensities in the emission spectrum of pyrene by co-immobilizing hydrophobic molecules (stearic acid), demonstrate energy transfer in the system of two spectrally overlapped chromophores (pyrene and perylene), and show quenching of pyrene fluorescence by ferrocene. Based on electrochemical measurements, the average distance between molecules for our interfaces is in the range of nanometers. The spatial separation of the coadsorbates is small enough to allow efficient communication within our monolayer assemblies. This fact is important from both fundamental and technological points of view, e.g., in the construction of sensors and design of nanoelectronic devices, and in understanding chemical deposition processes at heterogeneous interfaces.

Experimental Section

Chemicals. All chemicals were of the highest quality commercially available: 1-aminomethylpyrene hydrochloride (Aldrich, 95%), 1-aminopyrene (Aldrich, 97%), perylenedodecanoic acid (Molecular Probes), adipoyl chloride (Aldrich, 98%), 4-methylmorpholine (Aldrich, 99%), (aminopropyl)triethoxysilane (Aldrich), 1,6-pyrenedione (Aldrich), triethylamine (Aldrich, 99.5%), stearic acid (98+%), acetic anhydride

* To whom correspondence should be addressed. E-mail: Blanchard@chemistry.msu.edu.
[†] University of Warsaw.
[‡] Michigan State University.

10.1021/jp045323m CCC: $30.25
Published on Web 02/10/2005

(CCI, ACS grade), ferrocenecarboxylic acid (Aldrich, 97%), lithium perchlorate (Aldrich, 95+%), acetonitrile (Aldrich, anhydrous, 99.8%), and sulfuric acid (Aldrich, 99.999%). All other solvents used (pentanol, hexane, octanol, xylene, ethyl ether, toluene, 1-propanol, ethanol, chloroform, propionic acid, THF, methanol, ethylene glycol, DMF, water, and DMSO) were of spectroscopic grade. Aqueous solutions were prepared from water distilled in-house.

Steady-State Emission Spectroscopy. Emission and excitation spectra were recorded using a Spex Fluorolog 3 spectrometer set to a 3 nm band-pass for the excitation monochromator and a 3 nm band-pass for the emission collection monochromator.

Electrochemical Measurements. Electrochemical measurements were conducted with a PC-controlled Electrochemical Workstation (CH Instruments Model 604A), using a small-volume three-electrode cell with Pt wire as the counter electrode. All potentials are quoted vs a Ag/AgCl/3 M KCl_{aq} reference electrode.

Contact Angle Measurements. Contact angle measurements were done by placing a drop of HPLC water (volume ca. 15 μL) onto the investigated surface using a micropipet and recording several images of the water drop with a JVC digital camera.

Substrate Preparation. Quartz slides (NSG Precision Cells, Inc., P/N 10040 UV fused silica windows—nonfluorescent) and gold electrodes (Au, 99.99%; 0.2 cm^2) were cleaned by immersion in piranha solution for ca. 20 min. Indium-doped tin oxide (ITO) films (Bayview Optics, Dover-Foxcroft, ME) deposited on the same quartz slides were used for spectroscopic measurements and ITO films on glass substrates (Delta Technologies) were used for electrochemical measurements.

Bonding 1-Aminomethylpyrene to Quartz and ITO. Quartz and ITO substrates were reacted with adipoyl chloride (0.3 mL) in dry acetonitrile (10 mL), using 4-methylmorpholine (0.3 mL) as a Lewis base, under reduced pressure for ca. 30 min. The reacted substrates were removed from the reaction vessel, rinsed with dry acetonitrile and ethyl acetate, and dried under a stream of nitrogen. The acid chloride terminal functionalities were reacted with 1-aminomethylpyrene by exposing these substrates to a solution containing 1-aminomethylpyrene hydrochloride (0.03 g) and 4-methylmorpholine (1 mL) in dry acetonitrile (10 mL) for ca. 30 min. The reacted substrates were removed from the reaction vessel, washed with dry acetonitrile and ethyl acetate, and dried under a stream of nitrogen.

Bonding 3-Perylenedodecanoic Acid, Stearic Acid, and Ferrocenecarboxylic Acid to Quartz and ITO. Quartz and ITO substrates (with or without covalently bonded 1-aminomethylpyrene) were reacted with (3-aminopropyl)triethoxysilane (0.3 mL) in dry acetonitrile (10 mL), using triethylamine (0.3 mL) as a Lewis base, under reduced pressure for 2 h. The resulting silane-modified substrate was removed from solution, rinsed with acetonitrile, and dried. The terminal amino groups present on the substrate were reacted with the appropriate carboxylic acid-terminated moiety by exposing the substrates to a solution containing 3-perylenedodecanoic acid, stearic acid, or ferrocenecarboxylic acid (5 mM) and DCC (10 mM) in ethyl acetate for ca. 1.5 h. The substrates were then removed from the reaction vessel, washed with ethyl acetate, and dried under a stream of nitrogen.

Preparation of Thin Films of 1,6-Pyrenedione on Gold. 1,6-Pyrenedione thin films were prepared on gold by immersing gold-coated substrates into an acetonitrile solution of the compound (50 mM), followed by removal and drying. The resulting modified electrodes were characterized electrochemically in aqueous solution.

Preparation of 1-Amidopyrene Acetate. 1-Aminopyrene (0.5 g) was reacted with excess acetic anhydride (20 mL) in dry acetonitrile (20 mL) for ca. 20 h, resulting in the precipitation of amidopyrene acetate. The product was collected by filtration (yield 95%).

Preparation of 1-Amidomethylpyrene Acetate. 1-Aminomethylpyrene (0.5 g) was reacted with excess acetic anhydride (20 mL) in dry acetonitrile (20 mL) for ca. 20 h. The reaction mixture was poured into distilled water, which resulted in precipitation of amidomethylpyrene acetate. The product was then collected by filtration (yield 89%).

Results and Discussion

The goals of this work are to demonstrate communication between molecules bound to interfaces and to determine whether we can elucidate interactions between coadsorbates in complex monolayer structures.

The initial step is to attach fluorophores to the interfaces that are sensitive to the "polarity" of their surroundings, and observe their spectral response using steady-state emission spectroscopy. We use pyrene as a probe chromophore because of its well-established spectroscopic properties. At this point, it is appropriate to comment on the details of the pyrene emission "polarity" dependence. For this chromophore, the transition cross sections for the 0−0 emission band (the "1" band) and the emission band for the $S_0^{(v=1,b_{3g})} \leftarrow S_1^{(v=0)}$ transition (the "3" band) depend differently on the dielectric properties of the environment surrounding the chromophore. Specifically, the 1 band and 3 band are characterized by different vibronic coupling, with the vibronic coupling being mediated by the extent to which the *x*-polarized and *y*-polarized orthogonal singlet electronic state manifolds (S_1 and S_0) can couple. It is the vibrations of b_{3g} symmetry that couple these electronic states because such vibrations span both the *x* and *y* coordinates. Applying this phenomenon, Winnik et al. established the *Py* solvent polarity scale. The *Py* parameter for a given solvent is defined as the intensity ratio of the pyrene emission band 1 (at 375 nm) and the emission band 3 (at 384 nm) in the solvent.[20]

For dielectric-dependent differences in vibronic coupling to exhibit the strongest effect, the chromophore should be of D_{2h} symmetry, but when pyrene is substituted with an aliphatic moiety, the resulting perturbation to the excited electronic states is sufficiently small that dielectric mediation of inter-state vibronic coupling can still be seen. Such is the case for 1-aminomethylpyrene. The covalent attachment of the pyrene chromophore to the substrate, as discussed above, reduced the magnitude of the emission solvent-dependence, so the *Py* scale that was developed for pyrene will not apply directly. To gauge the diminution of this effect, we will examine the solvent-dependent emission behavior of several pyrene derivatives.

We have examined amidopyrene acetate[21] as a structural analogue of aminopyrene attached to the solid surface through an amide linkage. The solution phase emission spectrum of amidopyrene acetate in pentanol and hexane is shown in Figure 1a. Both emission spectra show three vibronic bands at 385, 402, and 425 nm which are substantially different from those of pyrene.[18] More significantly, we do not observe measurable differences in the spectra of 1-amidopyrene acetate taken in solvents of varying polarity. The absence of a solvent dependence is the result of the amide substituent on the pyrene ring system, which alters the excited electronic state structure and Franck−Condon factors compared to pyrene. This loss of

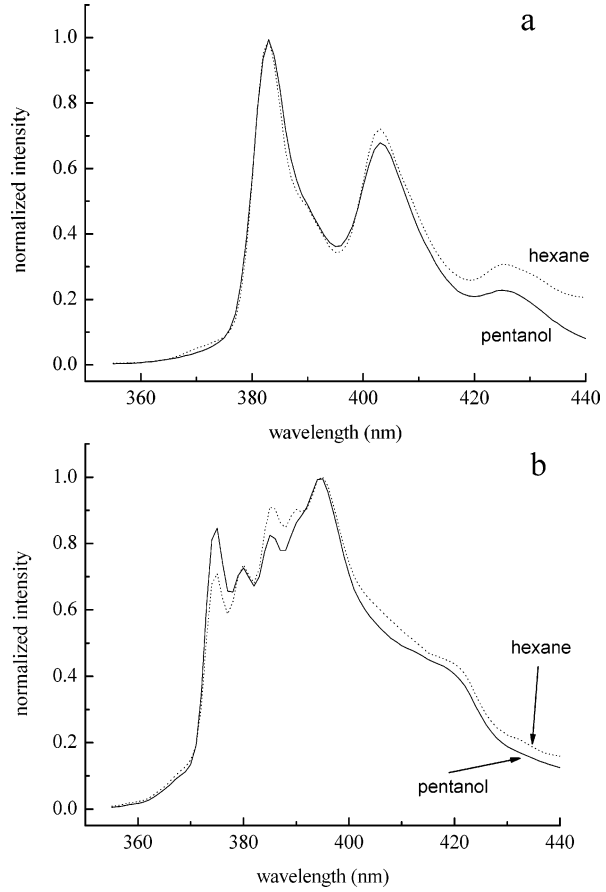

Figure 1. Emission spectra of (a) acetamidopyrene in pentanol and hexane and (b) acetamidomethylpyrene in pentanol and hexane.

solvent polarity sensitivity can be mitigated, however, by the separation of the amide functionality from the pyrene moiety by an aliphatic spacer, in this case a methylene group. We show in Figure 1b the solution phase emission spectra of amidomethylpyrene acetate in hexane and pentanol, revealing vibronic band structure similar to that of pyrene. We have confirmed experimentally that the ratio of the first (375 nm) and the third (385 nm) band is sensitive to the polarity of these solvents.

The experiments show clearly that we can use covalently bound aminomethylpyrene to probe the polarity characteristics of our interfaces. In Figure 2, parts a and b we present the excitation and emission spectra of aminomethylpyrene attached to an acid chloride-modified silica slide, immersed in water and hexane, respectively. We observe substantial changes in the relative intensities of the emission bands at 375 and 385 nm for immersion in these two solvents. In water, the I_1/I_3 band ratio is 1.53, and in hexane the I_1/I_3 band ratio is 0.64. In both spectra, the 385 nm emission band, which is well resolved for solution phase amidomethylpyrene acetate, is not as well resolved when bound to a substrate. This spectral change is possibly a consequence of fluorophore attachment to the surface, but a deeper understanding awaits further investigation. In terms of understanding environmental polarity, we note that the I_1/I_3 ratio changes linearly in correspondence to the *Py* parameter for a number of solvents for our samples containing the surface-bound chromophore (Figure 3). While the polarity-dependence of the I_1/I_3 band ratio is characterized by a smaller slope than that of the *Py* scale, surface-bound pyrene chromophores can clearly sense interface polarity in the same manner as the native pyrene chromophore.

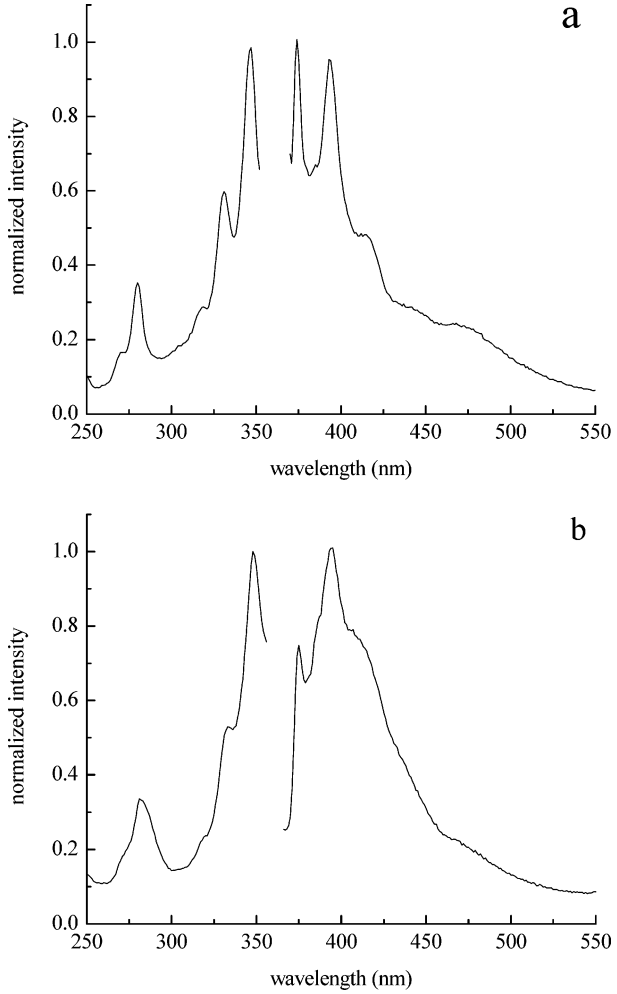

Figure 2. Excitation and emission spectra of (a) amidomethylpyrene adipate attached to quartz and the sample immersed in water and (b) amidomethylpyrene adipate attached to quartz and the sample immersed in hexane.

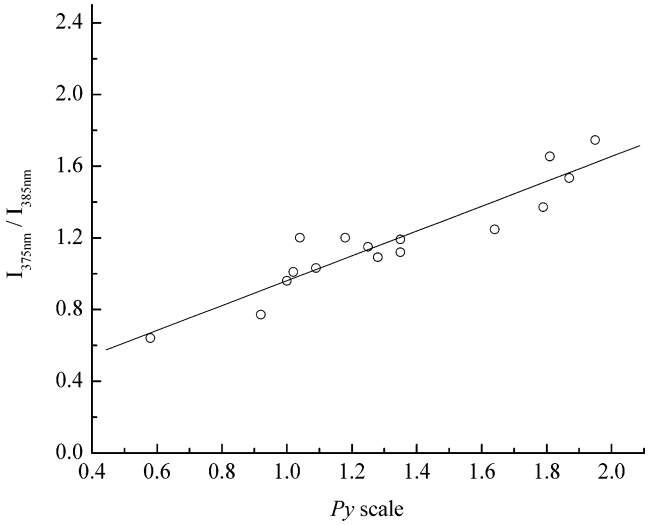

Figure 3. Dependence of the ratio of the emission intensities at 375 and 386 nm (for amidomethylpyrene adipate attached to quartz) recorded in a number of solvents versus *Py* scale value.

We turn our consideration next to the evaluation of the polar properties of the interface to which the molecule is attached. In Figure 4 (curve a) we show the emission spectrum (recorded in air) of aminomethylpyrene attached to a quartz substrate with adipoyl chloride. For this surface, the I_1/I_3 band ratio is rather

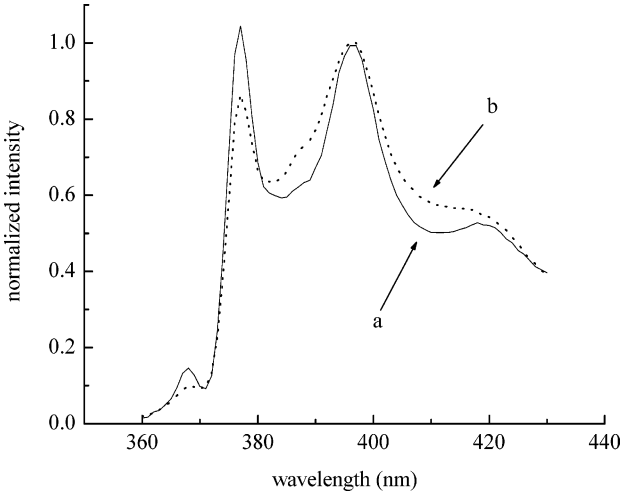

Figure 4. Emission spectra of (a) aminomethylpyrene attached to quartz (recorded in air) and (b) aminomethylpyrene and stearic acid co-attached to quartz (recorded in air).

high (1.66) indicating a polar interface. This is not a surprising result, since quartz is known to be relatively polar,[6] but the data do suggest that the interface possesses enough structural freedom such that the pyrene chromophore can be in close spatial proximity to the substrate (silanol or carboxyl) functionalities. Our data also indicate that the surface concentration of the pyrene chromophores is relatively low because we cannot resolve excimer emission (Figure 2a,b). The electrochemical measurements we report below (vide infra) substantiate this assertion. The immediate result of these findings is that the surface of our modified quartz substrates is hydrophilic, and surface contact angle measurements (ca. 48° for contact with water) support this assertion.

In an attempt to alter the polarity of these interfaces and at the same time evaluate the interactions of the pyrene chromophore with other adlayer constituents, we have synthesized several mixed interfacial systems: pyrene/stearic acid, pyrene/perylenedodecanoic acid, and pyrene/ferrocenecarboxylic acid (Scheme 1). The coadsorption of stearic acid was done to alter the polarity of the interface, the addition of perylenedodecanoic acid was done to alter polarity and determine the efficiency of intermolecular excitation transport, and the addition of ferrocenecarboxylic acid was done to demonstrate quenching of pyrene emission. This latter experiment was also prompted by recent work demonstrating the oxidative sensitivity of surface-bound polycyclic aromatic hydrocarbons.[15,22]

To create the pyrene/stearic acid two-component monolayer, we prepared a quartz substrate by attaching adipoyl chloride, then 1-aminomethylpyrene, as discussed above, then reacted the remaining surface silanol functionalities with aminopropyltriethoxysilane. The resulting aminated surface was reacted with stearic acid to create an amide linkage, using DCC as a coupling agent. We expect the co-attachment of stearic acid should increase the hydrophobicity of the interface, and indeed, the pyrene emission spectra reveal a decrease in the I_1/I_3 band ratio to 1.19 (Figure 4b) and an increase in the surface water contact angle to 66°. These results confirm our intuitive expectation that the attachment of the stearic acid moiety makes the interface more hydrophobic and verifies that the attached pyrene chromophore exhibits sufficient environmental sensitivity for our purposes.

In an effort to alter interface polarity and, at the same time, gauge the average distance between adsorbed species, we have synthesized interfaces containing two spectrally overlapped chromophores. We have bound perylenedodecanoic acid to interfaces already modified with the aminomethylpyrene functionality. We first bound aminomethylpyrene to the substrate using acid chloride chemistry, then reacted the resulting interface with aminopropyltriethoxysilane, then coupled perylenedodecanoic acid to the terminal amino functionalities. From a structural standpoint, we expect the pyrene and perylene chromophores to reside at different relative depths within the interfaces owing to the different lengths of the surface attachments. The perylenedodecanoic acid molecule is sufficiently hydrophobic to influence the emission profile of the co-attached pyrene chromophore, and our excitation and emission data demonstrate that intermolecular excitation transport is occurring at this interface (Figure 5). We have reported on the spectral characteristics of surface-bound perylene derivatives elsewhere,[22] and find its frequency-domain behavior to be very similar to that of solution phase alkylperylenes. The excitation and emission spectra of perylenedodecanoic acid attached to silica are shown in the inset to Figure 5.

We show in Figure 5 the excitation and emission spectral profiles of the silica substrate modified with both pyrene and perylene chromophores. The emission spectrum reveals the signals of pyrene (at 375 and 396 nm) and perylene (at 455 and 470 nm) while in the excitation spectrum, the bands at 285, 325, and 345 nm (pyrene) and 380, 415, and 430 nm (perylene) are both seen. In terms of the polarity of the interface local environment, we recover an I_1/I_3 band ratio for the pyrene chromophore of ca. 1.22, only slightly different than the stearic acid result and consistent with the perylene-modified interface being quite nonpolar.

We have excited the sample at 330 nm, coincident with the dominant absorption band of pyrene, and we observe an emission signal from both the pyrene and perylene derivatives. The intensity of the emission from perylene (peaks at 440 and 470 nm) is higher than that of pyrene (375 and 396 nm). On the other hand, when the sample is excited at 420 nm (coincident with the absorption band of perylene) we observe only the signals of perylene and no emission bands attributable to pyrene (Figure 6). This indicates that excitation transport from pyrene to perylene is efficient, or that the average distance between pyrene and perylene chromophores is on the order of the critical radius for this donor/acceptor pair.

For excitation spectra of this same sample (Figure 5), with emission collected at 480 nm (selective for perylene due to the absence of pyrene excimers), the perylene bands (380, 415, and 430 nm) are much smaller than the pyrene bands (285, 325, and 345 nm). This finding is fully consistent with the emission data and argues for the efficient transfer of energy between pyrene and perylene chromophores. We do not have absorption data on these interfaces, so cannot determine R_0 exactly from spectroscopic measurements, but a reasonable value for a variety of organic systems is $R_0 \sim 50$ Å.

To gain an estimate of the surface loading density of the chromophores, we use electrochemical measurements. Clearly such a measurement is not feasible on a silica surface, but cyclic voltammetry does provide a means for estimating surface loading density for interfaces grown on ITO substrates. In making these measurements, we tacitly assume the surface species concentrations on silica and ITO substrates are comparable. Both pyrene and perylene are electroactive, and based on their voltammetric behavior the surface coverage can be determined.

To estimate the surface loading of chromophores, we first need to consider their electrochemical behavior separately. We

SCHEME 1. Schematic Representation of Monomolecular Adlayers Studied[a]

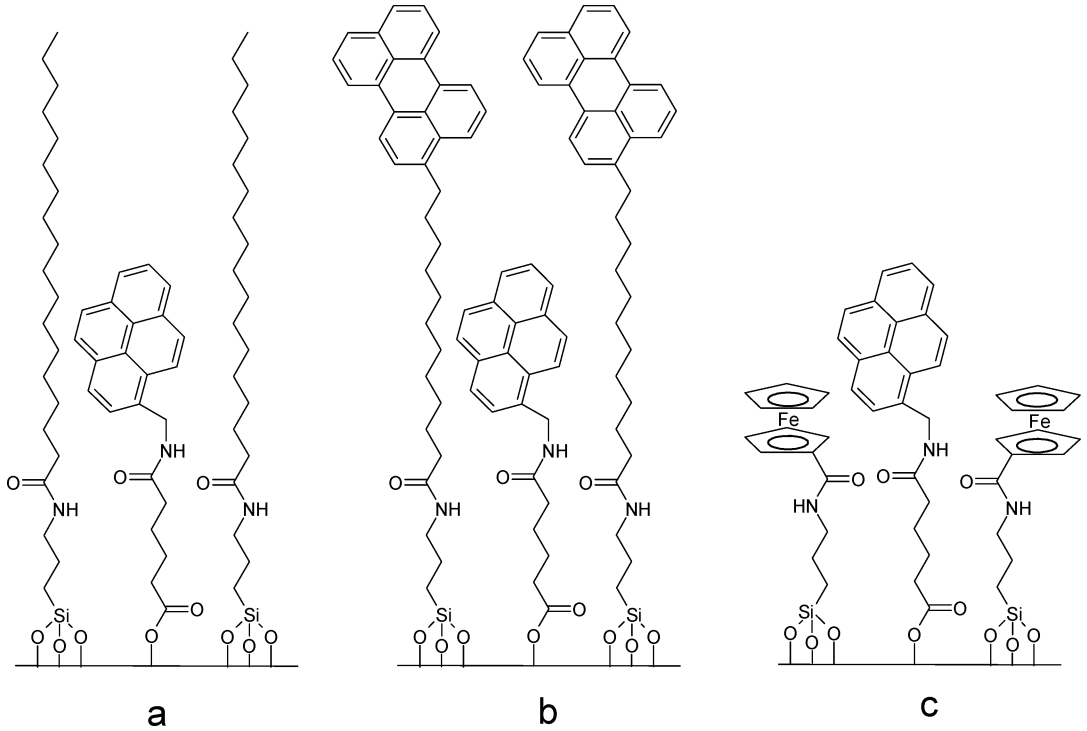

[a] Pyrene/stearic acid (a), pyrene/perylenedodecanoic acid (b), and pyrene/ferrocenecarboxylic acid (c).

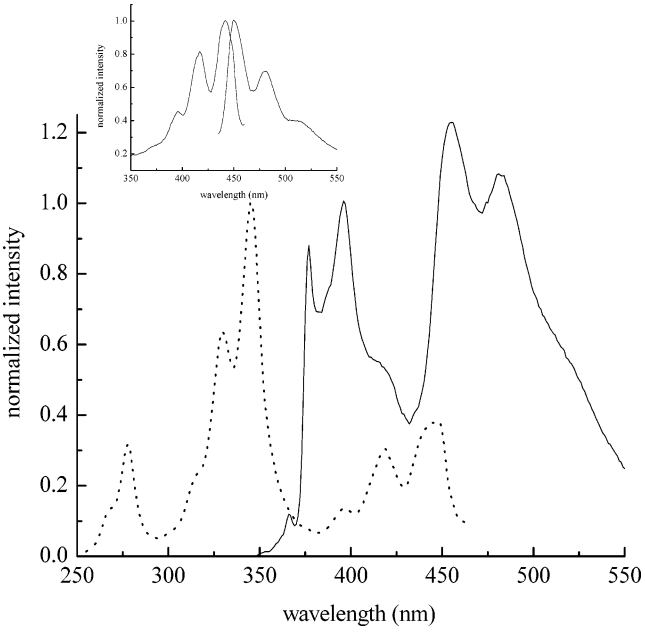

Figure 5. Excitation and emission spectra of pyrene and perylene co-attached to quartz (excitation wavelength: 330 nm). Inset: Excitation and emission spectra of perylene attached to quartz.

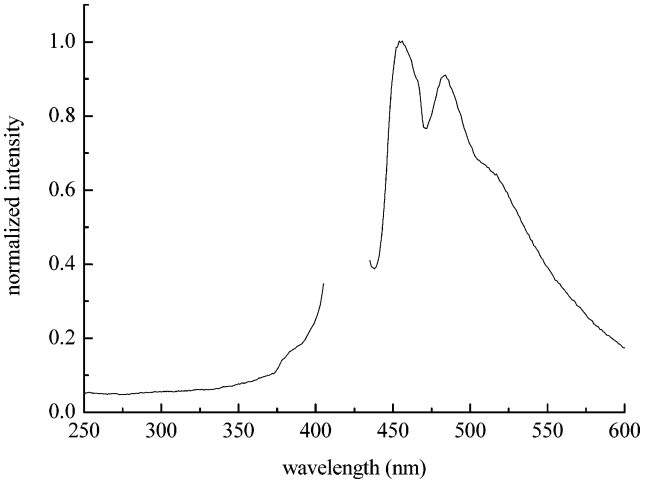

Figure 6. Emission spectrum recorded on quartz with co-attached pyrene and perylene (excitation wavelength: 420 nm).

show in Figure 7 a series of consecutive cyclic voltammetric curves of aminomethylpyrene attached to an adipate layer on ITO, recorded in aqueous sulfuric acid solution (0.5 M H_2SO_4). In the first scan we observe anodic current above 0.8 V, followed by the appearance of a new pair of peaks with a formal potential of 0.35 V. Qualitatively similar electrochemical behavior has been reported recently for amidopyrene hexanoate attached to ITO. In that work, we showed that the pyrene ring system is irreversibly oxidized to a radical cation, then subsequently transformed into a stable diol/dione redox couple.[15] Because we observe only one pair of peaks in the CV data we report here, we conclude that either there is only one stable isomeric form obtained or that the multiple isomeric forms are all characterized by the same redox potential. Comparing these data to those for the 1,6-pyrenedione/1,6-pyrenediol redox couple reveals remarkable similarity (Figure 7 inset). The similarity of these signals to the redox waves seen here indicates that the immobilized aminomethylpyrene is transformed into predominantly the same 1,6-pyrenedione/1,6-pyrenediol derivative. From this information we can estimate the surface coverage of pyrene bound to the ITO surface.[15,22,23] We can determine this quantity in a number of ways, but perhaps the most reliable method is to measure the charge exchanged during the quinone/hydroquinone reaction. First, we subtracted the baseline below the anodic peak, using the first scan as the baseline, and then integrated the current in the range 0.1−0.5 V. The potential axis was converted to time using the relationship $t = E/\nu$, to get the charge. Assuming a two-electron reaction, the surface

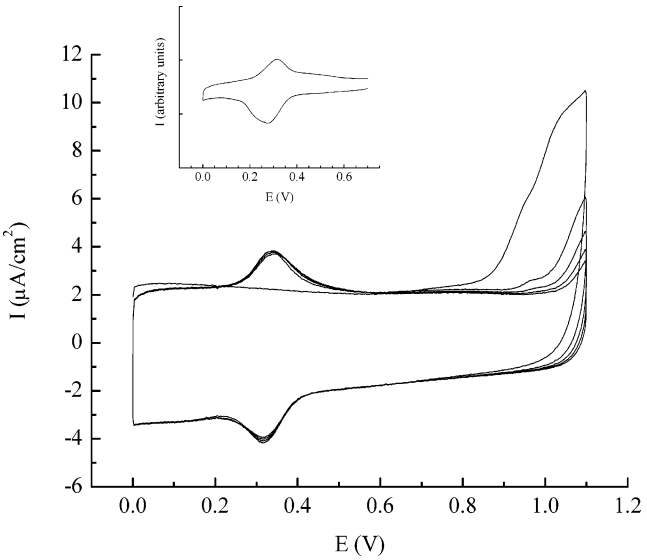

Figure 7. Consecutive cyclic voltammograms recorded in aqueous 0.5 M H_2SO_4 (sweep rate: 0.1 V/s) of aminomethylpyrene attached to ITO. Inset: Cyclic voltammogram of 1,6-pyrenedione physisorbed on gold.

concentration Γ can be determined according to the equation

$$\Gamma = \frac{Q}{2F} = 1.08 \times 10^{-11} \text{ mol/cm}^2$$

where Q is the charge (per cm^2) exchanged during the pyrenedione/pyrenediol reaction and F is the Faraday constant.

By way of comparison, a full monolayer for the alkanethiol/gold interface is ca. 7.7×10^{-10} mol/cm^2.[24] The value we obtain shows plainly that the bound pyrene moieties are not tightly packed; the average area per adsorbate molecule is ca. 15.4 nm^2. This finding accounts for the absence of excimer signal in the emission spectra and also provides an explanation for why further modification with triethoxyaminopropylsilane is feasible.

The electrochemical behavior of perylene is substantially similar and is described in detail elsewhere.[22] Perylene is oxidized irreversibly at 0.92 V to form a radical cation, which reacts with water to produce monohydroxy derivative(s) giving an unstable redox couple at 0.55 V. The monohydroxy derivative is further oxidized to form three isomeric redox couples of perylenediones/perylenediols with the redox signals at 0.19 V for 3,9-perylenedione/3,9-perylenediol, 0.23 V for 3,10-perylenedione/3,10-perylenediol, and 0.34 V for 1,12-perylenedione/1,12-perylenediol. A series of consecutive cyclic voltammograms of perylene attached to ITO is shown in Figure 8. Integration of the charge under the voltammetric peaks of perylenequinones allows calculation of surface loading density of the fluorophore which is 1.4×10^{-11} mol/cm^2.

With this characterization in hand, we now consider surface loading of both chromophores co-attached. In Figure 9 we present consecutive cyclic voltammograms of the oxidation of pyrene and perylene on the surface of ITO. In the first scan one observes a broad peak above 0.8 V, which corresponds to the oxidation of both pyrene and perylene. In subsequent scans some new signals appear: a transient pair at 0.55 V, which is monohydroxyperylene, and two stable redox couples at 0.35 and 0.19 V. The signal at 0.23 V matches the signals of the perylenedione/perylenediol couple and that at 0.35 V is likely a superposition of the signals of the dominant pyrenedione/pyrenediol isomer and one of the perylenedione/perylenediol isomers (with formal potential of 0.34 V, compare to Figure 8), which is much less intense. Since the electrochemical signals

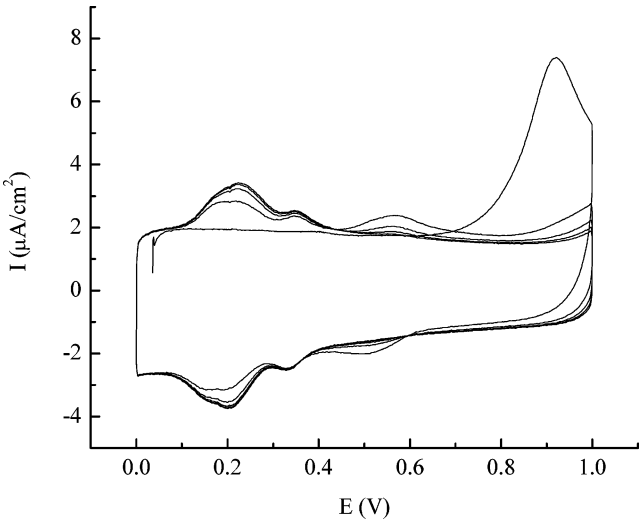

Figure 8. Consecutive cyclic voltammograms recorded in aqueous 0.5 M H_2SO_4 (sweep rate: 0.1 V/s) of perylenedodecanoic acid attached to ITO.

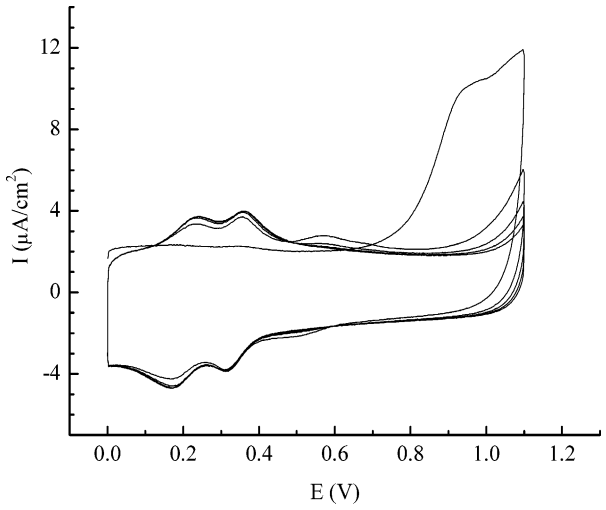

Figure 9. Cyclic voltammogram recorded on an ITO electrode with co-attached aminomethylpyrene and perylenedodecanoic acid; the sample was immersed in aqueous 0.5 M H_2SO_4. Sweep rate: 0.1 V/s.

overlap it is difficult do determine the correct concentrations of the chromophores. Calculating the charges under the redox peaks (dione/diol signals) and correcting the value for the presence of two kinds of species (pair at 0.35 V) we estimate that the molar ratio of pyrene and perylene on the surface is close to 1:1 and the total surface loading density of both chromophores is ca. 2.34×10^{-11} mol/cm^2. If we assume a statistical distribution of molecules on the surface the average distance between two chromophores is ca. 26 Å. It seems reasonable that such a distance is small enough to enable efficient energy transfer and other dipolar interactions between molecules.

As the third example of communication between surface-bound molecules, we studied pyrene/ferrocene adlayers. Ferrocene is known to quench the fluorescence of a variety of fluorophores, and we expect pyrene to be sensitive to this effect as well.[25−28] Co-attachment of ferrocene may be important also from a different point of view. As polycyclic aromatic hydrocarbons are known to undergo oxidative degradation when bound to interfaces, we intend to explore the possibility of using coadsorbed species (e.g., ferrocene) on such interfaces to spontaneously reduce any surface-oxidized species.

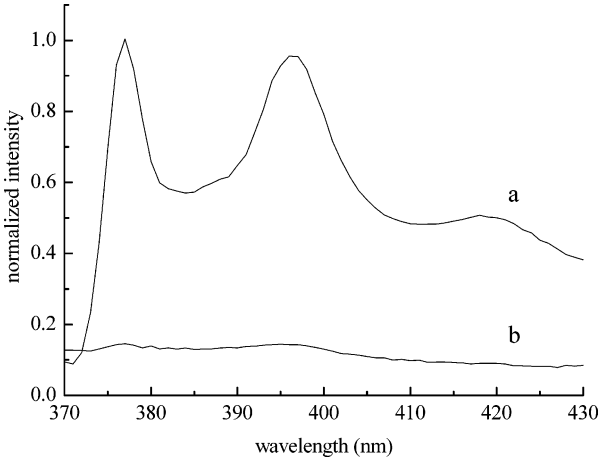

Figure 10. Emission spectra of (a) aminomethylpyrene attached to quartz (recorded in air) and (b) aminomethylpyrene and ferrocenecarboxylic acid attached to quartz (recorded in air).

The ferrocene functionality was deposited onto pyrene-containing substrates in the same manner as stearic acid and perylenedodecanoic acid. First, we have examined the spectral characteristics of the pyrene/ferrocene two-component adlayer on quartz (Figure 10). Intuition would suggest that the fluorescence signal of pyrene should be effectively quenched due to the addition of ferrocene to the surface. Indeed, we found experimentally that the intensity of the pyrene fluorescence signal was quenched to beneath the detection limit of our system. While it is not possible to evaluate surface polarity for this system (no signal), it is clear that the redox-active ferrocene moiety is in sufficiently close proximity to the chromophore to couple efficiently and induce quenching. This finding holds promise for the utility of ferrocene in reducing pyrene oxidation products (radical cations) once they form.

Since the reduction potential of pyrene is -2.09 V vs SCE[29] we believe that we can exclude the electron-transfer mechanism as a possible pathway of quenching. The free energy of electron transfer $\Delta G°$(ET) in this system can be estimated on the basis of the following equation:[29]

$$\Delta G°(\mathrm{ET}) = q(E_{(\mathrm{D}^+/\mathrm{D})}{}^0 - E_{(\mathrm{A}/\mathrm{A}^-)}{}^0) + E_{0-0}(\mathrm{pyrene}^*)$$

where q is the charge on the electron, the E terms are the indicated electrochemical potentials, E_{0-0} is the 0−0 transition energy for pyrene, D is an electron donor, and A is an acceptor. Assuming the value of ca. 3.35 eV for the excited-state energy of pyrene, we calculate $\Delta G°(\mathrm{ET}) = 6$ eV, a value that excludes the possibility of electron transfer from ferrocene to pyrene.

The mechanism of pyrene emission quenching for the pyrene/ferrocene system seems to be similar to that for the pyrene/perylene system. The absorption band of acetylferrocene (the analogue of ferrocene attached to quartz) is characterized by a maximum at 455 nm.[28] The spectral overlap between pyrene emission and ferrocene absorption is sufficiently high to allow efficient energy transfer, an effect manifested as the quenching of pyrene fluorescence. It is worthwhile to consider why the pyrene quenching is so efficient and we address this point by determining the average distance between molecules at the interface.

In an effort to estimate surface loading of both pyrene and ferrocene, we performed electrochemical experiments of ITO. The cyclic voltammogram of the pyrene/ferrocene electrode reveals characteristic signals for pyrene and relatively poorly shaped signals of ferrocene[30] at ca. 0.70 V (Figure 11). We

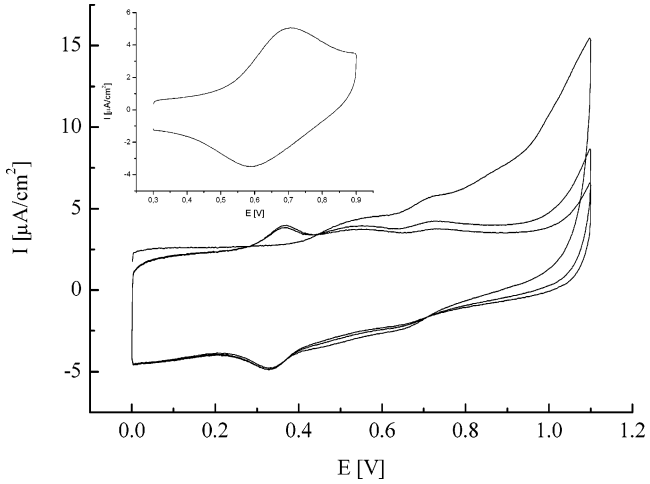

Figure 11. Consecutive cyclic voltammograms recorded on an ITO electrode with co-attached aminomethylpyrene and ferrocenecarboxylic acid; the sample was in aqueous 0.5 M H_2SO_4. Sweep rate: 0.1 V/s. Inset: Cyclic voltammogram recorded on an ITO electrode with co-attached aminomethylpyrene and ferrocenecarboxylic acid; the sample was immersed in 0.1 M $LiClO_4$ in acetonitrile. Sweep rate: 0.1 V/s.

rationalize the ferrocene signal form as follows. When ferrocene is oxidized and gains a positive charge, an anion from the electrolyte solution must enter into close proximity with the ferrocene to neutralize the charge. Because anions dissolved in aqueous medium are hydrated, the process of their transport into the hydrophobic region of the redox center is energetically unfavorable. Thus, some percent of ferrocene molecules are not oxidized simply because the associated anion transport is hindered. The analysis of the data yields a pyrene surface loading of 0.82×10^{-11} mol/cm^2. The value is lower than that seen when aminomethylpyrene is the only species bound to the ITO surface. We explain this finding on the basis that some tethered pyrene moieties are desorbed as a consequence of reacting the substrate to attach the ferrocene derivative.

We believe that only a fraction of ferrocene molecules are electrochemically active in aqueous solution, and have performed cyclic voltammetry in an organic solvent for comparison. We show in the inset to Figure 11 the cyclic voltammogram of an ITO substrate with co-immobilized aminomethylpyrene and ferrocenecarboxylic acid recorded in acetonitrile solution. The ITO electrode used for this experiment was not previously oxidized in aqueous medium. A pair of well-resolved voltammetric peaks is seen, attributable to the ferrocene redox reaction. We note that pyrene is not electroactive in this potential range (as indicated by the absence of pyrene voltammetric signals when ferrocene is not present; not shown). We calculate the ferrocene surface concentration to be ca. 5.3×10^{-11} mol/cm^2, which is significantly higher than that observed for perylene co-attached with pyrene. The reason for this finding is not clear but steric effects may induce higher reactivity of ferrocenecarboxylic acid with aminopropylsilane, in comparison to perylenedodecanoic acid.

For the ferrocene/pyrene surface, we calculate the average distance between molecules to be ca. 15 Å, significantly smaller than that for the pyrene/perylene system. This estimate explains qualitatively why the energy transfer and thus fluorescence quenching is so efficient for the ferrocene/pyrene interface.

Surface-bound pyrene can be used to monitor changes in polarity associated with the co-immobilization of other molecules, with the details of the pyrene optical response depending sensitively on the functionality coadsorbed to the interface. We have verified that interfacial polarity is modified by the addition

of either stearic acid perylenedodecanoic acid, and find that ferrocene serves as a remarkably efficient fluorescence quencher for tethered pyrene. In all cases, our data point to significant intermolecular communication between adsorbate species, and the combination of spectroscopic and electrochemical interrogation provides insight into the loading density and local environment(s) characteristic of these interfaces.

Conclusions

We have shown that aminomethylpyrene derivatives that are attached covalently to solid substrates such as quartz or ITO are indeed sensitive to their local environment, as manifested by the chromophore emission response. We have demonstrated the sensitivity of this effect using a series of interfaces with coadsorbed species, including an optical chromophore capable of participating in excitation transfer with the pyrene and an electrochemically active redox probe, which is shown to interact strongly with the surface-bound pyrene. We believe that this type of interface will be useful in probing processes such as chemical separations and interfacial dynamics.

Acknowledgment. We are grateful to the U.S. Department of Energy for support of this research through Grant DEFG0299ER15001.

References and Notes

(1) Ulman, A. *An Introduction to Ultrathin Organic Films*: Academic Press: New York, 1991.
(2) Ulman, A. *Chem. Rev.* **1996**, *96*, 1533.
(3) Dubois, L. H.; Nuzzo, R. G. *Annu. Rev. Phys. Chem.* **1992**, *43*, 437.
(4) Bain, C. D.; Troughton, E. B.; Tao, Y. T.; Evall, J.; Whitesides, G. M.; Nuzzo, R. G. *J. Am. Chem. Soc.* **1989**, *111*, 321.
(5) Bain, C. D.; Whitesides, G. M. *Angew. Chem., Int. Ed. Engl.* **1989**, *28*, 506.
(6) Keeling-Tucker, T.; Brennan, J. D. *Chem. Mater.* **2001**, *13*, 3331.
(7) Chen, S. H.; Frank, C. W. L. *Langmuir* **1991**, *7*, 1719.
(8) Spange, S.; Vilsmeier, E.; Zimmermann, Y. *J. Phys. Chem. B* **2000**, *104*, 6417.
(9) Hayashi, Y.; Kawada, Y.; Ichimura, K. *Langmuir* **1995**, *11*, 2077.
(10) Matsui, J.; Mitsuishi, M.; Miyashita, T. *Macromolecules* **1999**, *32*, 381.
(11) Fischer, K.; Spange, S.; Fischer, S.; Bellmann, C.; Adams, J. *Cellulose* **2002**, *9*, 31.
(12) Karpovich, D. S.; Blanchard, G. J. *Langmuir* **1996**, *12*, 5522.
(13) Kelepouris, L.; Krysiñski, P.; Blanchard, G. J. *J. Phys. Chem. B* **2003**, *107*, 4100.
(14) Krysiñski, P.; Blanchard, G. J. *Langmuir* **2003**, *19*, 3875.
(15) Mazur M.; Blanchard, G. J. *J. Phys. Chem. B* **2004**, *108*, 1038.
(16) Gao, L. N.; Fang, Y.; Wen, X. P.; Li, Y. G.; Hu, D. D. *J. Phys. Chem. B* **2004**, *108*, 1207.
(17) Kamat, P. V.; Barazzouk, S.; Hotchandani, S. *Angew. Chem., Int. Ed.* **2002**, *41*, 2764.
(18) Karpovich, D. S.; Blanchard, G. J. *J. Phys. Chem.* **1995**, *99*, 3951.
(19) Capek, I. *Adv. Colloid Interface Sci.* **2002**, *97*, 91.
(20) Dong, D. C.; Winnik, F. *Can. J. Chem.* **1984**, *62*, 2560.
(21) Kelepouris, L.; Krysinski, P.; Blanchard, G. J. *J. Phys. Chem. B* **2003**, *107*, 4100.
(22) Mazur, M.; Blanchard, G. J. *Langmuir*. In press.
(23) Mazur, M.; Blanchard, G. J. *Bioelectrochemistry*. In press.
(24) Kuwabata, S.; Fukuzaki, R.; Nishizawa, M.; Martin, C. M.; Yoneyama, H. *Langmuir* **1999**, *15*, 6807.
(25) You, C.-C.; Wurthner, F. *J. Am. Chem. Soc.* **2003**, *125*, 9716.
(26) Thornton, N. B.; Wojtowicz, H.; Netzel, T.; Dixon, D. W. *J. Phys. Chem. B* **1998**, *102*, 2101.
(27) Lee, E. J.; Wrighton, M. S. *J. Am. Chem. Soc.* **1991**, *113*, 8562.
(28) Giasson, R.; Lee, E. J.; Zhao, X.; Wrighton, M. S. *J. Phys. Chem.* **1993**, *97*, 2596.
(29) Manoharan, M.; Tivel, K. L.; Zhao, M.; Nafisi, K.; Netzel, T. L. *J. Phys. Chem.* **1995**, *99*, 17461.
(30) Krysiñski, P.; Brzostowska-Smolska, M.; Mazur, M. *Mater. Sci. Eng. C* **1999**, *8*−*9*, 551.